

Mémoire de Maîtrise en médecine No 54

Analysis of TRIP Expression in Different Types of Skin Tumor

Etudiant:

Noémie Arn

Tuteur:

Dr Marcel Huber

Service de dermatologie, CHUV

Expert:

Dr Thierry Roger

Service des maladies infectieuses, CHUV

Lausanne, janvier 2015

Abstract:

TRAF-interacting protein (TRIP) is a ubiquitously expressed nucleolar E3 ubiquitin ligase. Ubiquitination of proteins is a post-translational modification, which decides on the cellular fate of the protein. TRIP in vivo substrate has not been yet identified. However, TRIP has been shown to play an important role in cellular proliferation, especially in keratinocytes. TRIP was found to be up-regulated in basal cell carcinoma (BCC) at the mRNA level. This prompted us to elucidate its role in skin proliferative diseases such as cancer by analyzing its expression in BCCs at protein level and in squamous cell carcinoma (SCC) at mRNA and protein level. To that purpose, we performed a real-time PCR (qPCR) analysis followed by an immunohistochemistry (IHC) on formalin-fixed, paraffin-embedded (FFPE) biopsies.

The real-time PCR was performed on 12 RNA samples of which 6 were extracted from SCC biopsies and 6 from normal human skin. The results were statistically insignificant. Further analyses are needed on new RNA samples.

The IHC assay was performed on 20 biopsies from BCCs, 21 biopsies from SCCs and on 5 tissues from normal human skin. The results obtained showed an extensive expression of TRIP in keratinocytes nuclei. Due to various limitations related to the technique and to doubts about preservation of the antigens in the tissues from normal human skin, we could not highlight a clear difference in TRIP expression between the different tissues.

In conclusion, further analyses are needed on new RNA samples (qPCR) and on better preserved FFPE tissues from normal skin (IHC) to assess TRIP relative expression in BCCs and SCCs versus normal human skin.

Keywords: TRAF-interacting protein, TRIP, basal cell carcinoma, squamous cell carcinoma.

Table of Contents

1	INTRODUCTION	4
1.1	TRAF-INTERACTING PROTEIN	4
1.2	BASAL CELL CARCINOMA.....	5
1.3	CUTANEOUS SQUAMOUS CELL CARCINOMA	5
1.4	AIMS OF THIS WORK	6
2	RESULTS	7
2.1	REAL-TIME PCR.....	7
2.2	IMMUNOHISTOLOGY.....	10
2.2.1	<i>Antibody validation</i>	10
2.2.1.1	Western Blot	11
2.2.1.2	Immunofluorescence	13
2.2.2	<i>Immunohistochemistry</i>	15
2.2.2.1	Visual score	21
2.2.2.2	Computer assisted image analysis	23
2.2.2.3	IHC discussion	25
3	CONCLUSION	27
4	MATERIAL AND METHOD.....	27
5	BIBLIOGRAPHY	28

1 INTRODUCTION

1.1 TRAF-interacting protein

TRAF-interacting protein (TRIP) was initially identified to interact with Tumor Necrosis Factor Receptor –associated Factors (TRAF1 and TRAF2), and was reported to inhibit NF- κ B activation. Analysis of TRIP sequence revealed that TRIP is composed of an N-terminal RING finger motif, followed by coiled-coil and leucine zipper domains, both of which are implicated in protein-protein interactions (1). Subsequently, a study demonstrated that TRIP is a RING dependent E3 ubiquitin ligase which is able to undergo auto-ubiquitination (2).

E3 ligases carry out the final step in the ubiquitination cascade, catalyzing transfer of ubiquitin from an E2 enzyme to substrate (3). Ubiquitination is mostly known as a signal for proteasomal degradation but is also a signal for other cell processes such as DNA reparation, chromatin remodeling and cell signaling (4). The deregulation of several E3 ligases (such as BRCA 1, Mdm2, COP1) is known to be implicated in cancer development (5).

TRIP potential substrates are unknown (6). However, recent data showed that TRIP promotes ubiquitination of DNA polymerase η in humans cells and in *Drosophila* embryos which positively regulates this polymerase activity, suggesting that TRIP promotes proper cell cycle progression (7). Another potential substrate of TRIP is the TANK-binding kinase 1, whose proteasomal degradation is promoted by TRIP, therefore inhibiting IFN-beta signaling and the antiviral response (8).

Nopo is the *Drosophila* homolog of human TRIP. The alteration of its RING domain showed a lethal effect on *Drosophila* embryos, due to spindle defects, suggesting a role of Nopo in preservation of the integrity of the genomic integrity during early embryogenesis (9). Similarly, an attempt to generate TRIP knockout mice resulted in death of the animals during the embryonic development due to proliferation defects and excessive cell apoptosis (10). In human cells, TRIP E3 ligase activity was found to be functionally required for the spindle assembly checkpoint control (11).

Moreover, TRIP has been identified as interactor of CYLD through the C-terminal part of TRIP (12). CYLD is a tumor suppressor gene whose mutation is associated with familial cylindromatosis, a condition leading to the development of multiple skin appendages tumors (13). CYLD expression was found to be strongly down regulated in basal cell carcinoma (14). CYLD is a de-ubiquitinase that down regulates NF- κ B signaling (12), one consequence of this being the prevention of the transcription of cyclin D1 and, thus, inhibiting cell proliferation in keratinocytes (15). In human keratinocytes, CYLD over-expression increases epidermal differentiation and has the ability to decrease non-melanoma skin cancer progression and aggressiveness (16).

The tyrosine kinase SYK, a tumor suppressor, was also identified as a TRIP interactor. In breast epithelial cells, it has been shown that SYK and TRIP have opposing functions in the regulation of NF- κ B activity (17).

TRIP mRNA is expressed at low levels in a large number of mouse tissues (6). In human keratinocytes, TRIP mRNA expression levels are high in proliferating but low in differentiating cells (10). This has been shown to be regulated by PKC and the PI3K-Akt-mTOR pathway, both having an effect on the E2F family of transcription factors. In addition, knockdown of TRIP reduced proliferation rate of human keratinocytes and promoted the expression of differentiation markers such as keratin 1 and profilaggrin. Interestingly, these effects were not the result of an increased NF- κ B activity. Concerning other cells types, TRIP expression was found to be down regulated during the late stages of osteoclastogenesis (2). In human disease, TRIP level of expression was found to be increased in basal cell carcinoma (10). This expression level has not been studied in other types of skin tumors.

1.2 Basal cell carcinoma

Basal cell carcinoma (BCC) is the most common malignant cancer in individuals of mixed European descent. Its incidence is increasing due to aging of the population and sun exposure habits. BCC can be locally aggressive but does not normally metastasize (18).

BCCs display 5 major histological patterns: nodular, superficial, micronodular, infiltrating and sclerosing (=morpheic) which have different medical prognosis. Nodular and superficial BCCs can be removed by simple surgical excision in a high percentage of cases whereas the micronodular, the infiltrating and the sclerosing act more aggressive and have a higher risk of incomplete surgical removal (19).

Aberrant activation of the Sonic Hedghog signaling pathway plays a key role in the development of all types of BCC (18). The molecular pathogenesis leading to the different histological patterns of BCC is not well understood. Some data suggest that the magnitude of the Hedghog pathway activation may play a role for the tumor phenotype (20). Differences were found between the BCC types in expression level of different genes like nMyc (21) or genes associated with the MAP kinase pathway (22).

TRIP was found to be up regulated in BCC at the mRNA level (10), however its expression at protein level was never assessed.

1.3 Cutaneous squamous cell carcinoma

Cutaneous squamous cell carcinoma (SCC) is the second most common human cancer. The evolution of SCC is a process ranging from the precursor actinic keratosis to the SCC in situ, also called Bowen disease, invasive SCC and finally metastatic SCC (23). Histologically, the invasive SCC can be divided into three categories: the well, medium and poorly differentiated. Low degree of differentiation is associated to a higher risk of metastasis (24).

Unlike BCC, SCC pathogenesis is not associated with a specific signaling pathway. P53 mutations are found in 40% of SCCs. Aberrant activation of EGFR and Fyn are commonly found as well as activating mutations of the Ras oncogene (23).

TRIP expression in SCC is unknown.

1.4 Aims of this work

As TRIP seems to be implicated in cell proliferation and differentiation, especially in keratinocytes, a dysfunction in its expression could play a role in proliferative skin diseases such as cancer (10). An analysis of its expression in different skin tumors will help to understand the biological function of TRIP and its possible role in tumor genesis.

Regarding the fact that TRIP expression has not been analyzed in skin cancer types other than the basal cell carcinoma at mRNA level, the aim of this work is to analyze TRIP mRNA and protein level in biopsies from SCC and protein level in BCC. In order to do so, the chosen method was real-time PCR analysis followed by an immunohistochemistry on formalin-fixed, paraffin-embedded tumor tissues.

Considering that TRIP is down regulated during epidermal differentiation and that its knockdown repressed keratinocyte proliferation and enhanced differentiation, an expected result of this work could be the increased expression of TRIP in skin tumors. This is also consistent with the data showing the increased expression of TRIP at mRNA level in basal cell carcinoma (10).

2 RESULTS

2.1 Real-time PCR

The aim of this experiment was to measure TRIP relative expression at mRNA level in SCC versus normal human skin.

To that purpose, we used 12 total RNA samples of which 6 were extracted from SCC biopsies (sample 1 to 6) and 6 from normal human skin (sample 7 to 12).

The RNA samples were first reverse transcribed into cDNA. The cDNA was then analyzed in duplicate by real-time PCR. The target was TRIP and two housekeeping/normalizer genes, rpl13A and Tbp (endogenous control).

All the primers used in this experiment span exon-exon junctions in the target mRNA (=cross-intron primers) to prevent amplification of possible genomic DNA.

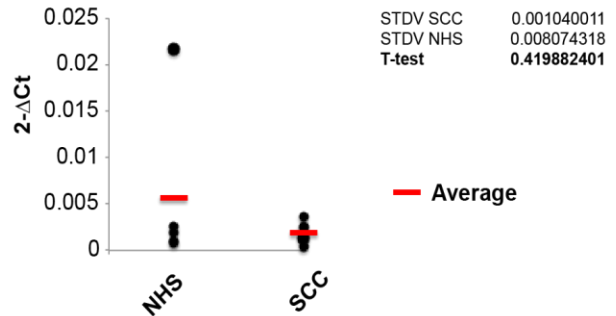
The results are shown in figure 1, following a comparative CT method, the $2^{-\Delta Ct}$ method (25). Statistical significance was calculated using students t-test.

For the $2^{-\Delta Ct}$ method to be valid, the amplification efficiencies of the target and the housekeeping gene must be approximately equal (25). If efficiencies are dissimilar, the ratio in Ct values of the target and the housekeeping gene will not be constant when the template amounts are varied. This assessment was already done for the need of other works in the laboratory.

Figure 1 - TRIP with RPL13 (A) and TBP (B) as normalizer genes – No template control (NTC) contains all the real-time PCR components except the cDNA, allowing the detection of contaminating nucleic acids.

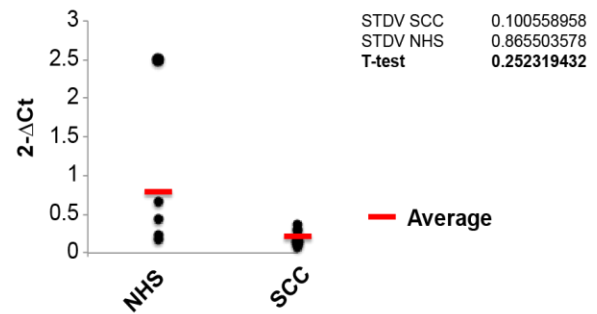
A

	Ct TRIP	Ct RPL13	ΔCt	2-ΔCt	
SCC	Sample 1	26.8781	18.2314	8.6467	0.00249508
SCC	Sample 2	28.3337	16.9468	11.3869	0.00037342
SCC	Sample 3	27.1136	17.5997	9.5139	0.00136783
SCC	Sample 4	27.2647	18.5956	8.6691	0.00245664
SCC	Sample 5	27.7715	18.422	9.3495	0.00153292
SCC	Sample 6	29.153	21.0613	8.0917	0.00366569
NHS	Sample 7	no amp.	no amp.		
NHS	Sample 8	29.9639	21.3291	8.6348	0.00251574
NHS	Sample 9	35.3621	29.8378	5.5243	0.02172801
NHS	Sample 10	27.9341	18.0682	9.8659	0.00107169
NHS	Sample 11	28.8496	18.731	10.1186	0.00089949
NHS	Sample 12	27.9914	18.9455	9.0459	0.00189196
NTC	no amp.	no amp.			
NTC	no amp.	no amp.			



B

	Ct TRIP	Ct TBP	ΔCt	2-ΔCt	
SCC	Sample 1	26.8781	25.075	1.8031	0.28655818
SCC	Sample 2	28.3337	24.83	3.5037	0.08816195
SCC	Sample 3	27.1136	24.277	2.8366	0.13999042
SCC	Sample 4	27.2647	25.56	1.7047	0.30678503
SCC	Sample 5	27.7715	24.955	2.8165	0.14195445
SCC	Sample 6	29.153	27.668	1.485	0.35724853
NHS	Sample 7	no amp.	no amp.		
NHS	Sample 8	29.9639	29.356	0.6079	0.65615111
NHS	Sample 9	35.3621	36.682	-1.3199	2.49648805
NHS	Sample 10	27.9341	25.793	2.1411	0.22670687
NHS	Sample 11	28.8496	26.3276	2.522	0.17410144
NHS	Sample 12	27.9914	26.822	1.1694	0.44460621
NTC	no amp.	no amp.			
NTC	no amp.	no amp.			



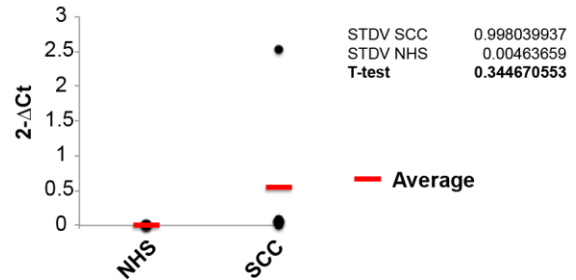
This experiment shows a fold change in TRIP expression of -2.83 in SCC versus NHS using the RPL13 normalizer gene and of - 3.63 using the TBP normalizer gene. However, the Student's t-test is statistically insignificant in both cases ($p > 0.05$).

The use of cross-intron primers do not provide full protection against amplification of contaminating genomic DNA. Considering the possibility of such a contamination, the RNA samples were treated by DNase digestion. After this digestion, RNA concentration was measured by NanoDrop, revealing very low concentration in some samples. RNA was reverse transcribed into cDNA. Several qPCR were performed using RPL13, TBP and RPL0 as normalizer genes (Figure 2).

Figure 2 – postDNase digestion – TRIP with RPL13 (C), TBP (D) and RPL0 (E) as normilizer genes.

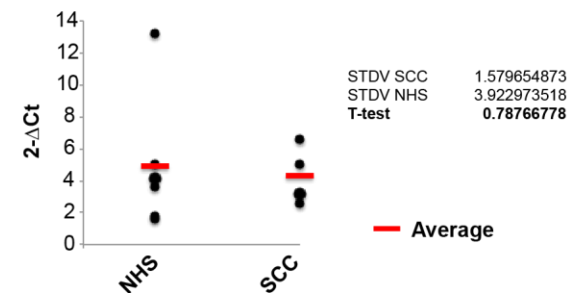
C

	Ct TRIP	Ct RPL13	ΔCt	2-ΔCt	
SCC	Sample 1	26.49	21.924	4.566	0.04221794
	Sample 2	29.453	23.369	6.084	0.01474122
	Sample 3	28.139	23.33	4.809	0.03567358
	Sample 4	30.595	31.938	-1.343	2.5367828
	Sample 5	29.066	25.349	3.717	0.07604515
	Sample 6	no amp.	no amp.		
NHS	Sample 7	33.03	22.798	10.232	0.0008315
	Sample 8	32.116	23.802	8.314	0.00314222
	Sample 9	26.766	19.875	6.891	0.00842563
	Sample 10	29.336	22.457	6.879	0.008496
	Sample 11	26.53	18.899	7.631	0.00504476
	Sample 12	25.819	19.784	6.035	0.0152505
NTC	32.294	no amp.			
NTC	37.027	36.71			



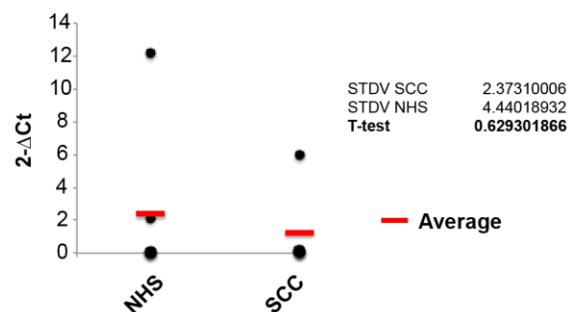
D

	Ct TRIP	Ct TBP	ΔCt	2-ΔCt	
SCC	Sample 1	26.49	29.21	-2.72	6.58872814
	Sample 2	29.453	30.823	-1.37	2.58470566
	Sample 3	28.139	29.807	-1.668	3.1777376
	Sample 4	30.595	no amp.		
	Sample 5	29.066	31.4	-2.334	5.04201357
	Sample 6	no amp.	no amp.		
NHS	Sample 7	33.03	33.7	-0.67	1.59107297
	Sample 8	32.116	35.843	-3.727	13.2415491
	Sample 9	26.766	28.801	-2.035	4.09822729
	Sample 10	29.336	31.19	-1.854	3.61501091
	Sample 11	26.53	27.393	-0.863	1.8188165
	Sample 12	25.819	28.153	-2.334	5.04201357
NTC	32.394	no amp.			
NTC	37.027	no amp.			



E

	Ct TRIP	Ct RPL0	ΔCt	2-ΔCt	
SCC	Sample 1	26.49	21.67	4.82	0.03540262
	Sample 2	29.453	23.843	5.61	0.0204749
	Sample 3	28.139	24.658	3.481	0.0895601
	Sample 4	30.595	33.177	-2.582	5.98769195
	Sample 5	29.066	25.342	3.724	0.07567707
	Sample 6	no amp.	no amp.		
NHS	Sample 7	33.03	34.109	-1.079	2.11257125
	Sample 8	32.116	35.723	-3.607	12.1847099
	Sample 9	26.766	22.86	3.906	0.06670783
	Sample 10	29.336	22.687	6.649	0.00996441
	Sample 11	26.53	17.578	8.952	0.0020192
	Sample 12	25.819	21.234	4.585	0.04166558
NTC	32.394	35.29			
NTC	37.027	36.11			



The results we find in figure 2 are again statistically non significant. Due to big 2-ΔCt variations in some samples, it was difficult to display the results in a graph in a readable manner.

As we can see, fold changes in TRIP expression vary depending on the housekeeping gene used.

The expression of housekeeping genes is presumed to be stable within the samples extracted from SCCs and normal skin tissues.

RPL13A, TBP and RPLO are all housekeeping genes who are commonly used in studies of gene expression in keratinocytes (26). However, no universal housekeeping gene with proven invariable expression between experimental conditions has been yet identified (27). Therefore, the validity of a housekeeping gene should be evaluated before analysis of expression of other gene. This was not done in this experiment. Hence, we cannot exclude that the results found in this experiment were biased by the fact that the expression of the housekeeping genes used here were not stable between the different mRNA samples, especially in the ones extracted from SCC.

Moreover, we cannot assure that the SCC biopsies from which the RNA was extracted did contain a high proportion of tumor tissue. Indeed, tumors can be histologically very heterogeneous and contain large amount of non tumoral tissue, like immune cells. Unlike BCCs, SCCs do not have a known quantifiable marker that we could have use as a control.

Furthermore, we cannot exclude a partial degradation of the RNA samples during the DNase digestion process. Indeed, concentration of nucleic acids in some samples was very low after this process and sample 6 could not be amplified anymore.

Therefore, relative quantification of TRIP mRNA in SCC could not be determined by this experiment.

2.2 Immunohistology

Evaluation of gene expression at mRNA level is a vital initial step but is insufficient. Studies have shown that there is often discordance between levels of nucleic acids and proteins, implying that the study of both measures is important (28). Immunohistochemistry (IHC) on formalin-fixed, paraffin-embedded (FFPE) tissue is a widely used technique to assess protein expression. It allows preservation of morphology of tissues. FFPE are easy to store, can be conserved over a long time and can therefore be easily obtained for a study. However, the limitations of IHC are numerous. It involves a series of steps which can all affect the reliability of the results.

2.2.1 Antibody validation

Before the IHC can be started, the first critical step is to determine the validity of the antibody designed for the experiment.

To be validated, an antibody needs to recognize the antigen of interest in a specific and reproducible manner (29).

We had two anti-TRIP antibodies that were candidates for the IHC experiment, the Abcam ab 151307 (next rabbit anti-TRIP) and the Abcam ab 4533 (next goat anti-TRIP). Both are polyclonal antibodies. The rabbit anti-TRIP is generated against a recombinant fragment of

TRIP and the goat anti-TRIP against a synthetic peptide. To determine the specificity of those antibodies, we performed a Western Blot, followed by an immunofluorescence on cultured cells lines.

Antibody reproducibility means good correlation between different antibody lots. Different lots can show different staining patterns (29). The question of reproducibility was not tested in this work as we did only use one lot of each antibody.

2.2.1.1 Western Blot

7 cultures of 293 T cells (human embryonic kidney) were transfected with several plasmids using the CaCl transfection method according to the next table:

Table 1 (ug/ul DNA)

Plasmid	1	2	3	4	5	6	7
<i>pmycTRIP</i>	2.4	2.4	2.4	2.4	2.4	2.4	2.4
<i>MT742</i>		1.2			2.4		
<i>MT743</i>			1.5			3	
<i>pSHC2</i>				1.95			3.9
<i>pGEM-11Zf+</i>	2	1	1	1			
<i>pEGF-N3</i>	0.2	0.2	0.2	0.2	0.2	0.2	0.2

The 7 cultures were transfected with plasmids containing TRIP attached to a Myc tag. A plasmid containing a fluorescent tag pEGF-N3 was also transfected to each culture.

MT742 and MT743 are both shRNAs targeting TRIP. pSHC2 is the negative control of MT742 and MT743. pGEM-11Zf+ is a standard cloning vector.

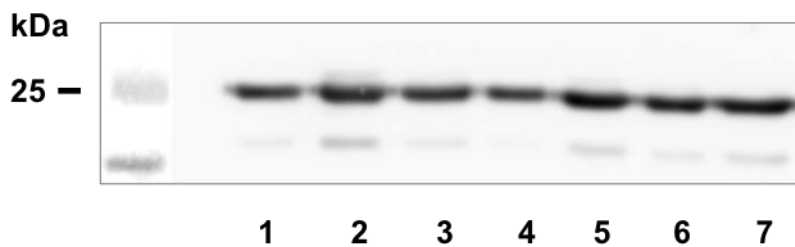


Figure 3: anti-GFP

As we can see, the transfection was successful in all cultures. The differences in protein quantity may be due to loading irregularity or variances in transfection efficiency between the 7 cultures. Ideally, a homogenously expressed gene like actin should have been used as a loading control.

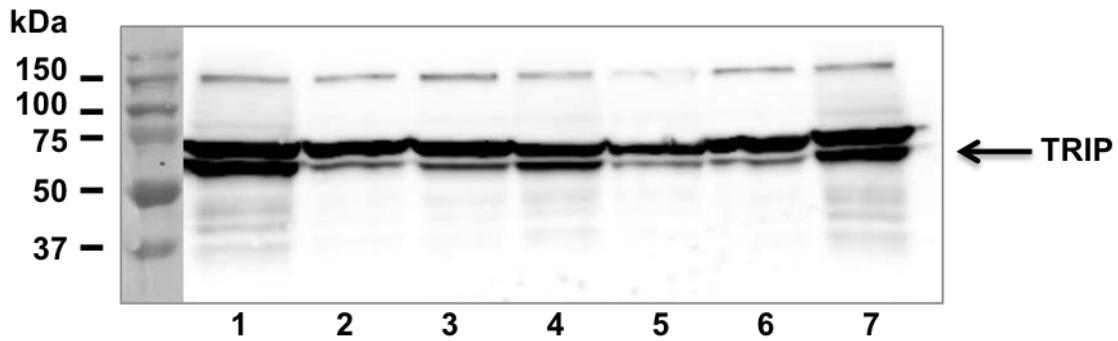


Figure 4: rabbit anti-TRIP

TRIP is a 53 kDa protein. In figure 4, two lines can be seen between the 50 kDa and the 75 kDa markers. Cultures 2, 3, 5 and 6 are expected to express less TRIP because there were transfected with inhibitors. This pattern is observed in the line underneath. The line above may be due to unspecific binding of the antibody or to its binding to an ubiquitinated TRIP.

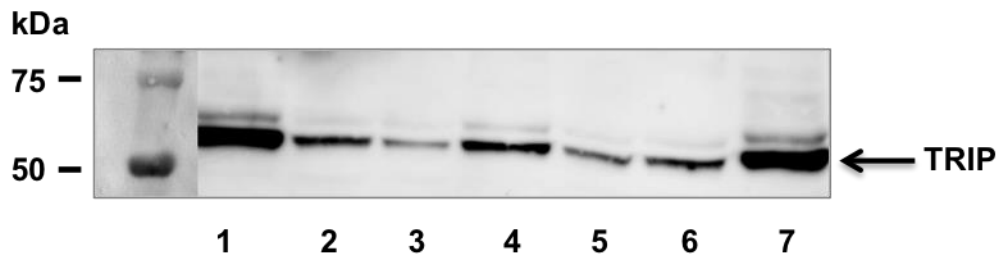


Figure 5: goat anti-TRIP

Figure 5 shows one line above the 50 kDa marker, suggesting a specific binding of the goat antibody to TRIP protein.

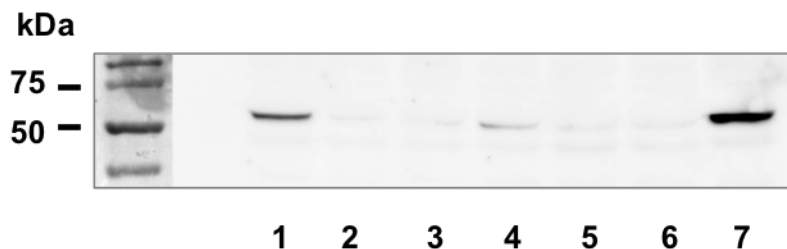


Figure 6: anti-Myc

Figure 6 shows the positive control using a specific anti-myc antibody which makes the tag attached to TRIP apparent. The second line seen in figure 2 cannot be found here. It could be caused by post-translational modifications or degradation of TRIP which make the Myc-Tag unrecognizable. However, we cannot exclude an unspecific binding of the rabbit anti-TRIP with this experiment.

Furthermore, the two antibodies we tested were generated against a synthetic peptide/recombinant fragment of TRIP and not against a purified protein. Those peptides/recombinants do not necessarily recognize the 3D structure or the post-translational modifications of the native protein (29). Therefore, the tested antibodies may bind to the denatured TRIP in the WB but not to the native conformation of TRIP that is found in fixed tissues.

2.2.1.2 Immunofluorescence

As we saw, a WB is not a sufficient test to validate an antibody designed to bind to an IHC because of the denaturation of the antigens. Therefore, an immunofluorescence (IF) may be useful to investigate the specificity further.

In this experiment, we transfected 3 HeLa cells cultures with a plasmid containing TRIP attached to a FLAG-tag. After two days of growth, the cultured cells were fixed in paraformaldehyde and an IF was performed using DAPI for fluorescent staining of the DNA. During the IF, the 3 cultures were incubated each with another primary antibody: one with the rabbit anti-TRIP, one with the goat anti-TRIP and one with a rabbit anti-FLAG.

Unfortunately, the cells incubated with the goat anti-TRIP and the anti-FLAG tag were probably degraded during the fixing process and the results of the IF were non interpretable in both cases.

In Figure 7 and 8, we can see the results for the culture incubated with the rabbit anti-TRIP.

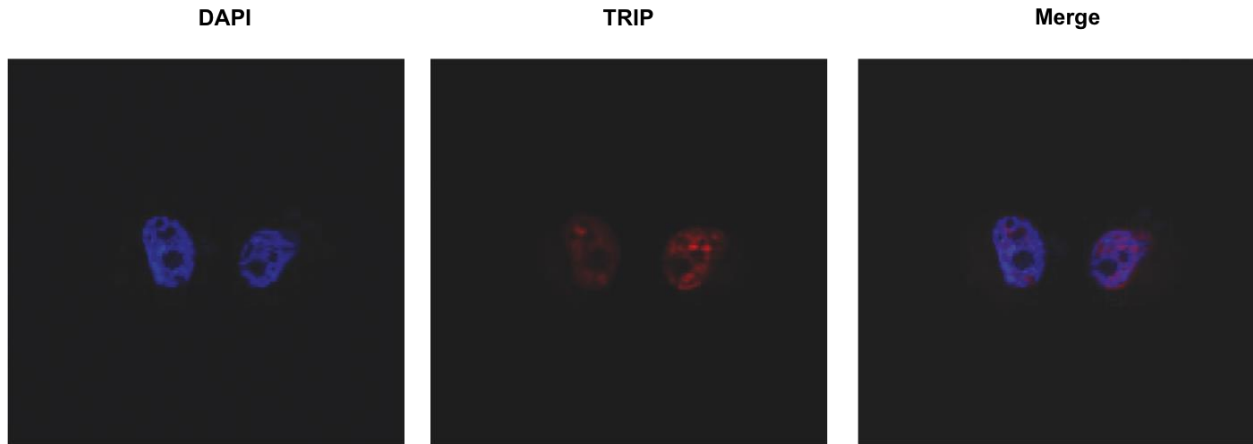


Figure 7: rabbit anti-TRIP 1:300

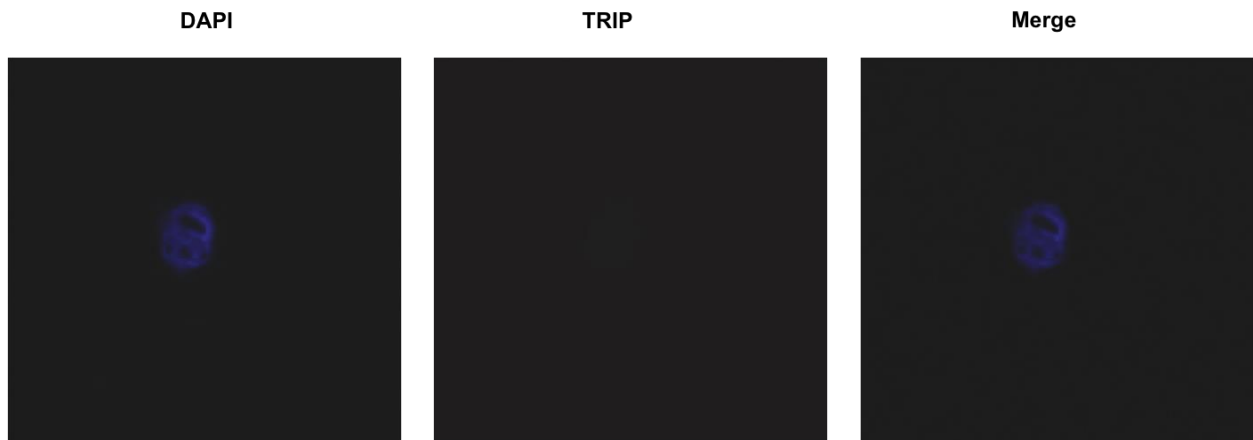


Figure 8: rabbit anti-TRIP - negative control (no primary antibody)

The blue signal emitted by DAPI highlights the nucleus. The red signal shows indirectly the rabbit anti-TRIP. As we can see in figure 7, the blue and the red signals are perfectly superimposed which implies that the rabbit anti-TRIP reacts with an antigen located in the nucleus.

Figure 8 is the negative control where the cells were only incubated with the secondary antibody but not with the rabbit anti-TRIP. As expected, there's no red signal.

TRIP is a protein known to be located in the nucleus (11). We demonstrate here that the rabbit anti-TRIP detects a nuclear antigen which may assist the specificity of the antibody.

Unfortunately the culture incubated with the anti-FLAG tag (attached to TRIP) was degraded and could not be interpreted. Therefore, a control is lacking to investigate if the FLAG tag and the TRIP signal have similar cellular location, which would be a further argument in favor of the rabbit anti-TRIP specificity.

After this experiment, it was decided to choose the rabbit anti-TRIP for the immunohistochemistry on FFPE tumor tissue.

2.2.2 Immunohistochemistry

To continue the analysis of the expression of TRIP protein, we decided to perform IHC to 4 different types of BCC: the infiltrating (INF), nodular (NOD), superficial (SUP) and sclerosing (SCL) types.

Concerning the SCC, we divided the biopsies into four categories: the Bowen disease, the well- (BD), the medium- (MD) and the poorly- (PD) differentiated.

The classification of the biopsies between the different categories was based on the medical pathological reports of the hospital department of dermatology of the CHUV.

Initially we had the following biopsies available which we cut into 5 µm sections:

Table 2 – number of biopsies for the IHC

BCC biopsies				
	INF	NOD	SCL	SUP
Ordered	5	6	6	7
Excluded	1	2	1	0
Total	4	4	5	7
SCC biopsies				
	Bowen	BD	MD	PD
Ordered	5	7	10	9
Excluded	0	2	3	5
Total	5	5	7	4

As seen in table 2, we decided to exclude several biopsies before the beginning of the experiment. The biopsies excluded were either too small to see a sufficient quantity of tissue or were empty of any cell.

To evaluate TRIP expression in normal skin, we had several paraffin slices from human foreskin, scalp, abdomen and face as well as a biopsy from shoulder skin.

The first attempts to perform an IHC on the sections were very unsuccessful with high nuclear and cytoplasmic staining, suggesting unspecific binding of the antibody (picture not shown). The experimental conditions had to be optimized to get a satisfying result. In particular, the primary antibody dilution and incubation time turned out to be crucial to obtain a seemingly specific signal. The antigen retrieval was performed by an acidic heat-induced technique. However, with some sections, we got better results with a pH 9 antigen retrieval (Tris-EDTA, TE).

The results we got were rather heterogeneous and sometimes contradictory. Hence, it was quiet challenging to interpret and to summarize them in this work.

IHC is a semi-quantitative method, whose interpretation can be addressed by different ways. The first question asked is to know if a specific staining is present or not. If so, in what percentage of cells is it present, that is to say the extent of staining. Another question concerns the intensity of staining.

Those questions can be approached by different methods such as visual scoring systems and image analysis by computer software. Visual scoring systems rely on the experience and acuity of the eye of the observer and are therefore subject to inter-observer variability (30).

In the literature, data has been showing that image analysis by software can be a suitable alternative (31-33) and could as well be time effective (34) and have better sensitivity (35).

In this work, we decided to try both approaches, as shown in sections 2.2.2.1 and 2.2.2.2.

As numerous sections were stained, it's was not possible to show them all in this work. A selection can be seen in figure 9, 10, 11 and 12. Please note that this selection is not clearly representative of all slides.

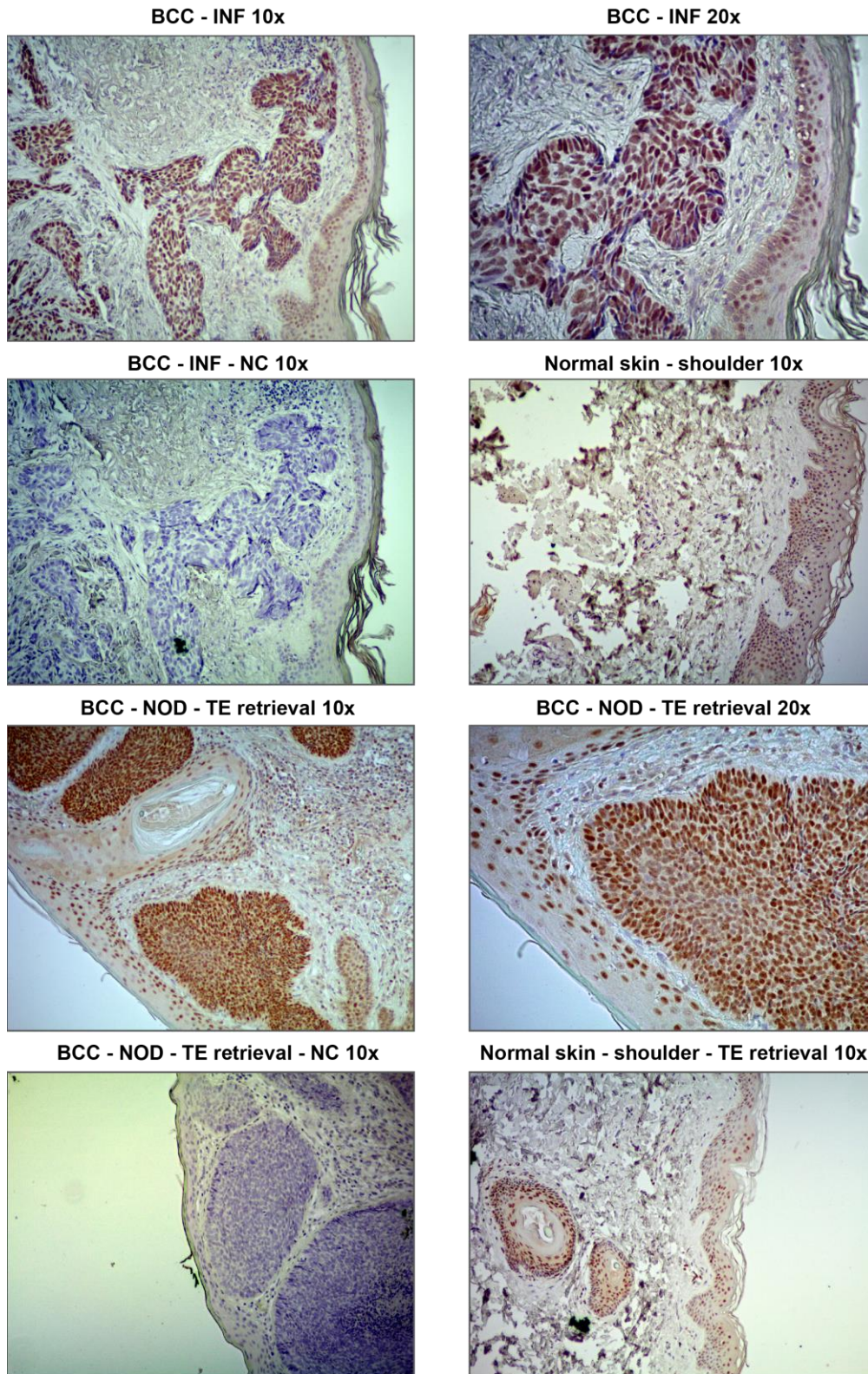


Figure 9 – NC: negative control without primary antibody. TE: antigen retrieval by pH 9. INF: infiltrative BCC. NOD: nodular BCC.

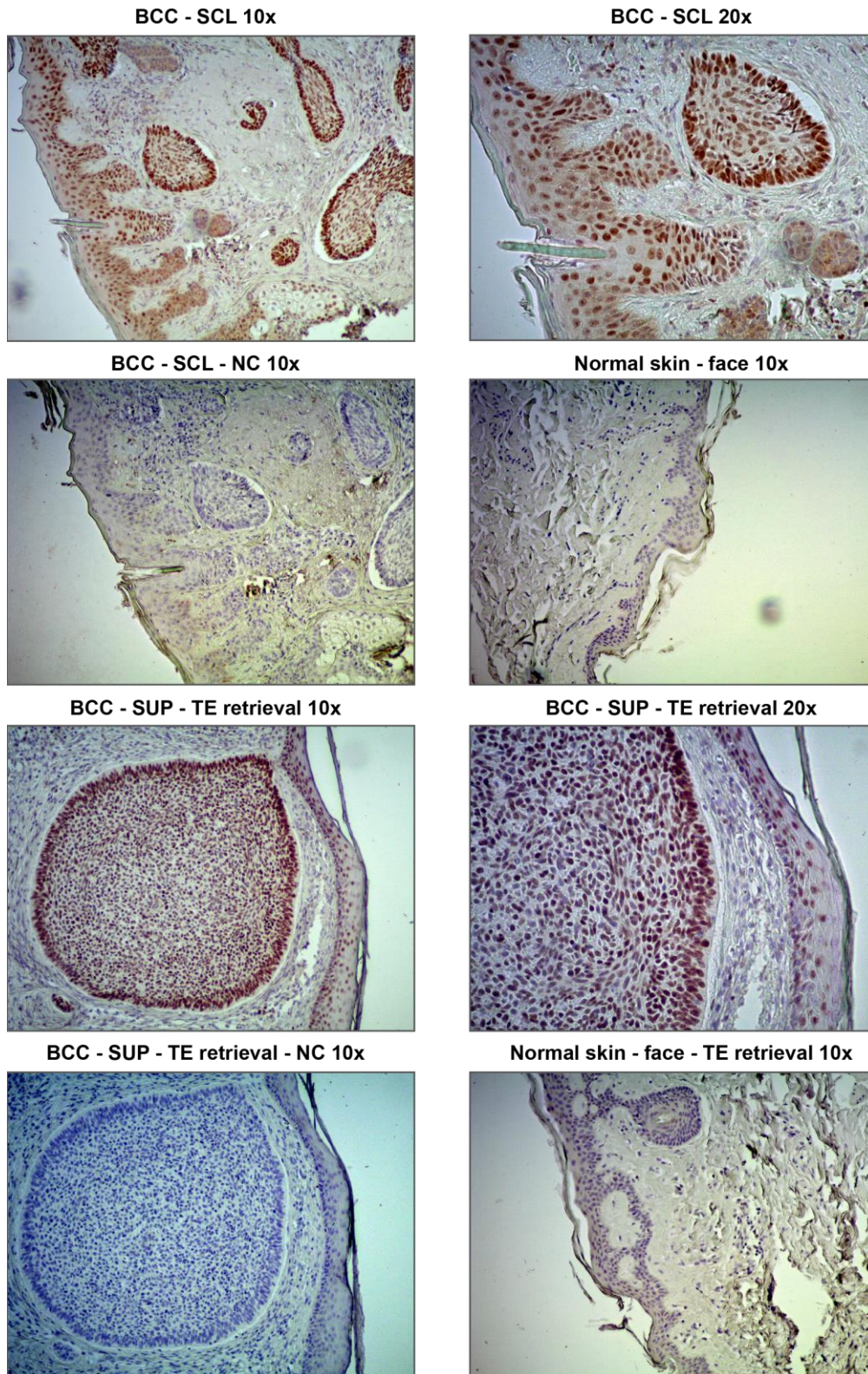


Figure 10 – NC: negative control without primary antibody. TE: antigen retrieval by pH 9. SCL: sclerosing BCC. SUP: superficial BCC.

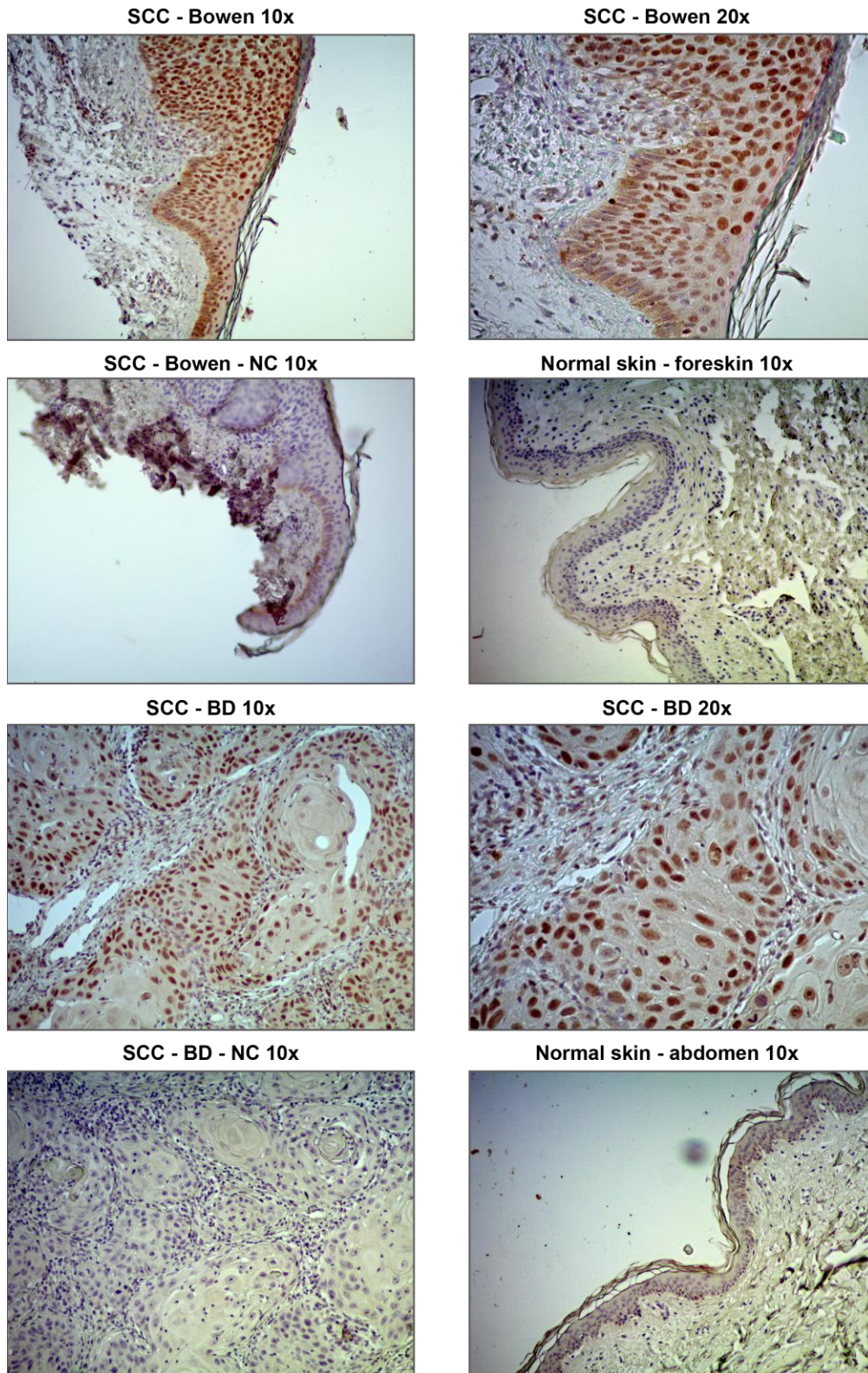


Figure 11 – NC: negative control without primary antibody. BD: well differentiated SCC.

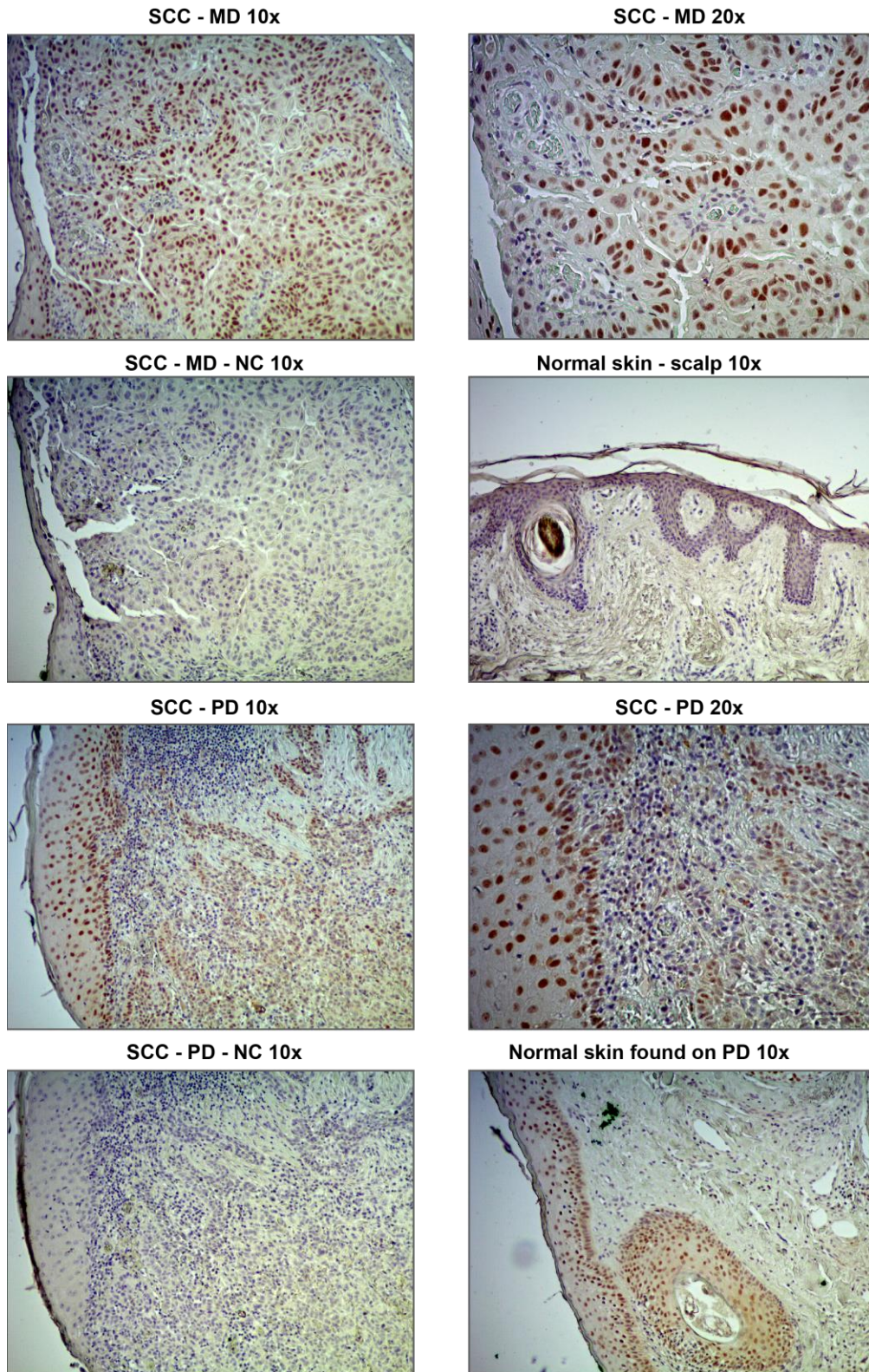


Figure 12 – NC: negative control without primary antibody. MD: medium differentiated SCC. PD: well-differentiated SCC.

As we can see, there's a clear nuclear staining pattern with rather low background. In tumor tissue, a vast majority of nuclei are stained which suggests that TRIP is extensively present. Negative controls with no primary antibody all resulted in negative immunoreactivity. In normal skin, staining is absent or almost absent except in the shoulder skin biopsy where TRIP expression looks slightly lower than in most tumors tissues, regarding the extent and intensity of staining.

2.2.2.1 Visual score

We choose to apply a visual score based on the Quick score (37) where proportion of stained cells as well as the intensity of staining are taken into consideration. This score works as followed:

Proportion of stained cells:	Score	Staining intensity:	Score
no nuclear staining	0	no staining	0
< 1% nuclear staining	1	weak staining	1
1-10% nuclear staining	2	moderate staining	2
11%-60% nuclear staining	3	strong staining	3
61 – 90 % nuclear staining	4		
90 % - 100% nuclear staining	5		

The proportion and the intensity scores are then added. Therefore, minimal score is 1 and maximal is 8. Only nuclear staining was considered. A minimum of 100 cells were counted for each case.

Regarding TRIP expression in normal skin, we did analyze the staining in normal skin sections (table 6) but also on pieces of normal skin that we identified on tumor slides (table 7). Normal skin was not found on each slide.

Table 3 – Visual score on SCCs

	Proportion of stained cells	Intensity of staining	Total score
Bowen 2	5	3	8
Bowen 3	5	3	8
Bowen 4	5	3	8
Bowen 5	5	3	8
BD1	5	2	7
BD2	5	2	7
BD4	5	2	7
BD6	4	2	6
BD7	5	3	8
MD2	5	2	7
MD3	4	2	6

MD5	4	2	6
MD7	5	2	7
MD8	5	2	7
MD9	5	2	7
MD10	5	2	7
PD4	5	2	7
PD7	5	1	6
PD8	5	2	7
PD9	4	1	5

Table 4 – Visual score on BCCs

	Proportion of stained cells	Intensity of staining	Total score
INF1	5	2	7
INF2	5	3	8
NOD4	5	2	7
SCL4	4	2	6
SCL5	5	2	7
SCL6	5	2	7
SUP1	5	2	7
SUP2	4	1	5
SUP3	5	2	7
SUP4	5	3	8
SUP5	4	2	6
SUP6	4	3	7

Table 5 – visual score on BCCs retrieved by TE

	Proportion of stained cells	Intensity of staining	Total score
INF4	5	3	8
INF5	5	3	8
NOD1	5	2	7
NOD5	5	3	8
SUP7	4	2	6

Table 6 – visual score on normal human skin. TE refers to the antigen retrieval method

	Proportion of stained cells	Intensity of staining	Total score
Abdomen	1	2	3
Shoulder	4	2	6
Shoulder TE	4	2	6
Face	1	0	1
Face TE	2	1	3
Foreskin	1	0	1
foreskin TE	1	0	1
Scalp	1	0	1

Table 7 – visual score on normal skin identified in tumor biopsies

	Proportion of stained cells	Intensity of staining	Total score
INF 3	4	1	5
NOD 4	5	3	8
SCL 4	5	3	8
SUP7	4	2	6
BOW2	5	2	7
BOW3	5	2	7
BOW4	4	2	6
BD1	4	2	6
BD2	4	1	5
MD8	5	3	8
BD4	5	2	7
BD6	5	2	7
MD9	5	3	8
PD1	5	2	7

As we can see, the score of most of the tissues lie between 6 and 8, except in normal skin where lower scores are found. However, the normal skin visualized on pieces of tumor has similar scores as tumor tissues.

The proportion of stained cells being very high in almost all tissues, comparison between the tissues relies almost completely on the intensity assessment, which is less objective.

2.2.2.2 Computer assisted image analysis

Most current imaging systems rely on standard color cameras, employing a red-green-blue Bayer-pattern. Those systems distinguish between chromogens present in the picture and do unmix them to quantify them separately. In practice, unmixing the DAB brown color from the haematoxylin blue color works fine (30).

However, the color value may vary significantly depending on the camera, the camera chips and the illumination source (30).

We choose to use the IHC Profiler, an open-source plugin compatible with Image J (38). This plugin can detect either cytoplasmic or nuclear markers. Basically, the IHC profiler works by creating a selection in areas with brown pixels. The threshold of pixel detection can be manually optimized, so that all nuclei are included in the selection, even the unstained ones. The IHC profiler will then undergo a pixel-per-pixel analysis of the selection and the brown pixels are divided into 4 categories of intensity: negative, low-positive, positive, high positive.

For this analysis, we selected pieces of picture that did contain high amount of the tissue of interest. The selection was then analyzed by IHC profiler. As with the visual score method, the slides that we are comparing were not necessarily stained during the same day but were all processed with the same standardized protocol.

Results are shown in figure 13 and 14.

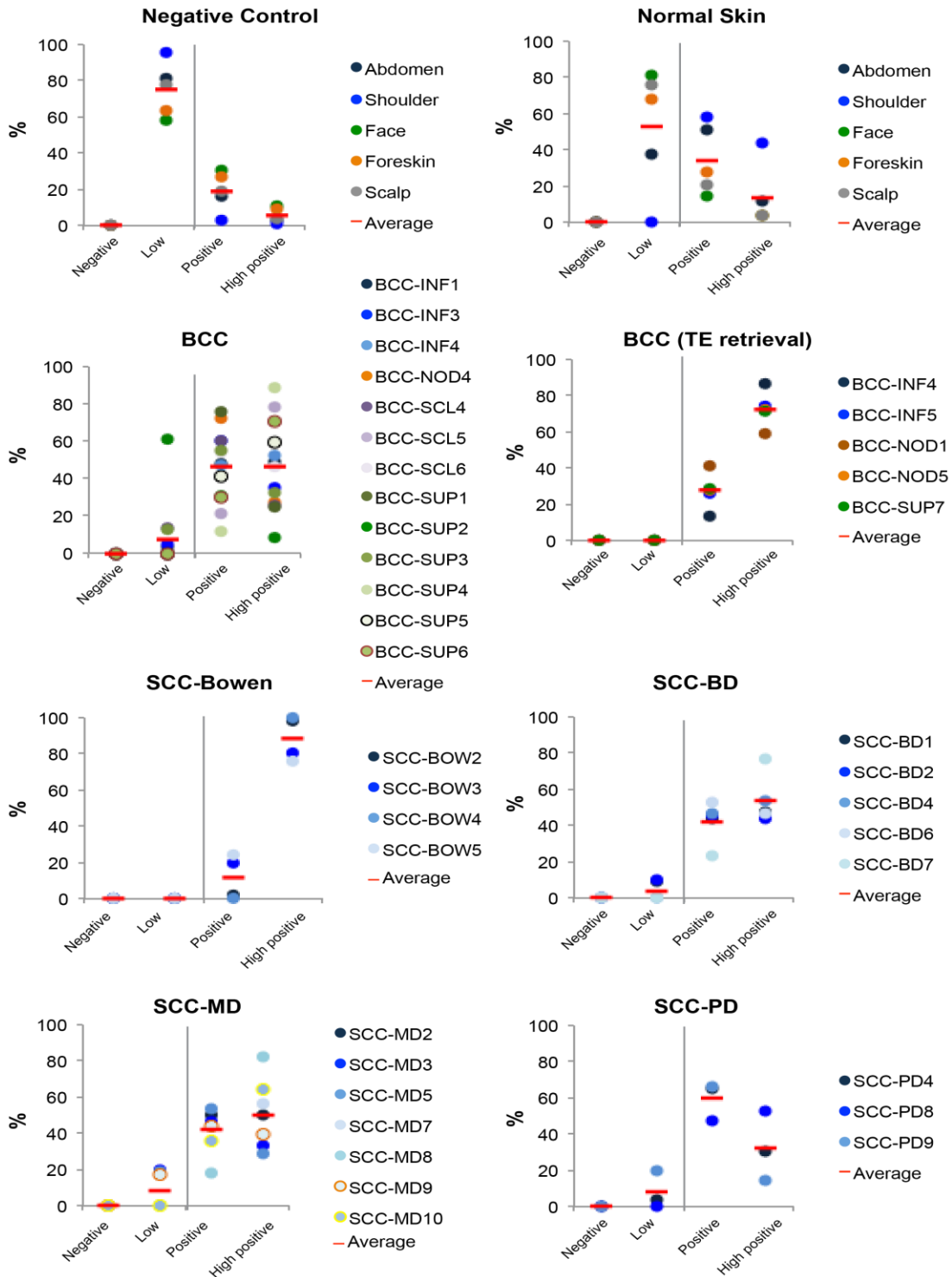


Figure 13 – DAB brown staining is divided into four categories of intensity: negative, low, positive and high positive. The vertical axes are showing the percentage of pixels in each category from the total pixels in each biopsy.

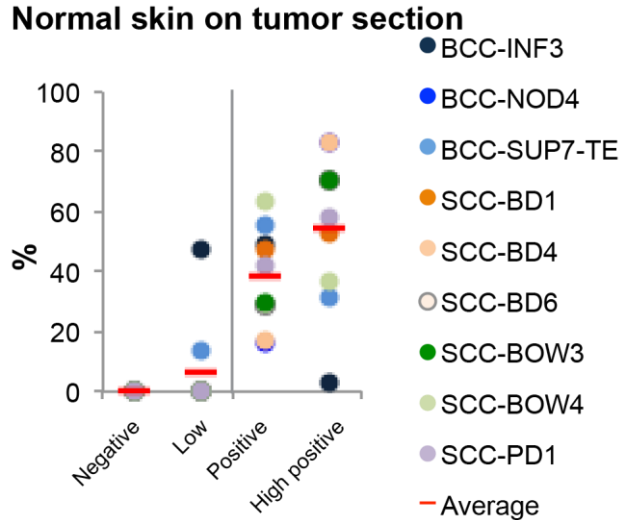


Figure 14 - DAB brown staining is divided into four categories of intensity: negative, low, positive and high positive. The vertical axes are showing the percentage of pixels in each category from the total pixels in each biopsy.

As seen in figure 13, the IHC profiler detects low signal even in the negative control which were not showing any staining. This is probably due to a background caused by low quality of our pictures. Therefore, we consider that negative and low positive intensity are both corresponding to absence of staining.

The tissues showing the highest proportion of high intensity signal are the Bowen disease, which is consistent with their visual score. Interestingly, in SCCs, the lower the degree of differentiation, the lower the intensity of the signal. This is also somehow consistent with the visual score.

The intensity pattern is clearly lower in the normal skin compared to tumor tissues.

However, figure 14 show the intensity pattern of normal skin found on tumors sections and there is no clear difference between this pattern and the one from the tumors.

The results obtained with IHC profiler are not to be over interpreted for reasons concerning the quality of pictures as well as other limitations that we will discuss next. However, we think that it is as useful tool to represent a synthesis of the experiment which contained more than 50 tissues, allowing a brief overview.

2.2.2.3 IHC discussion

The major limitation of IHC is its recurrent lack of reliability and reproducibility which can be affected by improper optimization in each step of the experiment.

A common cited problem is the fixation process. The time necessary for fixation depends on size and type of tissue and is often uncontrolled (30). Typically, this can lead to “patchy” staining, which we did encounter during the processing of some BCCs sections.

Another critical step in IHC is the antigen retrieval which can affect both intensity and extend of staining. The microwave used for the retrieval in this experiment did not allow a precise control of the temperature neither a homogenous heating of the solution containing the slides. This may have affected the homogeneity of the results, especially when comparing slides which were not stained during the same day.

An important limitation of this experiment was the lack of a proper normal skin control. Indeed, all the normal skin tissues we had were inadequately stocked (the shoulder biopsy being an exception) and therefore cannot be interpreted. Consequently, we had to search for pieces of normal skin in the tumor slides to have something to compare. Those pieces could possibly contain molecular defects and are not necessarily completely healthy.

Concerning IHC interpretation, the extent of the staining is easier to assess than the intensity which is more subjective. Staining was found in a vast majority of keratinocytes nuclei. Therefore, the only way to compare the slides between each other was the intensity of staining which makes the interpretation more delicate. In that matter, the IHC profiler turned out to be useful.

Ideally, if intensity of staining is being assessed, there should be a positive control, having different levels of staining intensity to compare to. Such control was lacking in this work. Furthermore, it is important to point out that the intensity of DAB staining is not perfectly correlated to the amount of antigen. The relation between both is only linear at low levels of antigen (39). However, data suggest that TRIP is expressed at low level (6) which is consistent with the high Ct obtained during the real-time PCR.

In this experiment, absence of staining or very low staining was found on the normal skin sections except on the shoulder biopsy. This correlates with TRIP mRNA in normal tissue reported to be low (6). However, this absence of staining cannot be interpreted as low expression of TRIP in those tissues. Indeed, the slides were cut several years ago. Proteins are known to be relatively stable in entire FFPE biopsies but are more sensitive to degradation once sliced. Consequently, sections should ideally not be stained more that several months after their cutting (36). Therefore, we suspect the absence of staining in the face, foreskin, scalp and abdomen tissues to be the consequence of protein degradation by improper stocking. Indeed, TRIP staining was quiet strong in normal skin from the shoulder biopsy (which was fresh cut) and on pieces of normal skin found on tumor sections. Therefore, an important limitation of this experiment was the lack of a proper normal skin control.

Altogether, we could not highlight a clear difference in TRIP expression between the different tissues. If a difference exists, we are assuming that it is a relative minor one which is difficult to assess in a semi-quantitative manner.

3 CONCLUSION

The aim of this work was to analyze TRIP expression in BCC and SCC tumors. The measure of this expression at mRNA level by real-time PCR did not show interpretable results.

The IHC experiment seems to have detected TRIP presence in a specific manner and showed an extensive expression of TRIP in keratinocytes. Due to numerous limitations related to the technique and experiment conditions, it was not possible to determine the relative expression of TRIP between tumor and normal skin tissue.

Consequently, further analyses are needed. The next step could be to perform a real-time PCR on new RNA samples. Those samples could be extracted from FFPE biopsies, the latter being more easily available than frozen biopsies. To isolate tumor cells from other type of cells, laser micro-dissection on FFPE sections prior to the RNA extraction could be considered.

4 MATERIAL AND METHOD

Cell culture

293 T and Hela cells were cultured in DMEM containing 10% fetal bovine serum.

Plasmids

E. Coli were cultured in a Lysogeny-broth medium containing 100 mg/ml of ampicillin and used as a host for the plasmids production.

Plasmid DNA isolation was carried out using QIAGEN Spin Miniprep Kit (QIAGEN) as per the manufacturer's protocol.

Transfections

293 T cells were transfected in CaCl₂ 2M and HBSS buffer.

HeLa cells were transfecting using jetPRIME transfection kit as per the manufacturer protocol.

Synthesis of cDNA and real-time PCR

RNA was purified using the RNeasy Kit (Qiagen) and its concentration was measured by NanoDrop spectrophotometer. cDNA was synthesized using Primescript-RT Kit (TakaRa). Quantitative PCR analysis was performed with Power SYBRGreen PCR Mastermix (Applied Biosystems).

Western Blot

Proteins were extracted by cell lysis in 1% SDS in phosphate-buffered saline and quantified using the Pierce BCA Protein Assay Kit. For immunoblots, the following antibodies were used: anti-TRAIP antibody (Abcam 151307 and Abcam 4533), anti-rabbit HRP-linked antibody

(NA934V, GE healthcare) and anti-goat HRP-linked antibody (sc-2020, Santa Cruz Biotechnology). Signal from immunoblots were captured by using LAS4000.

Immunofluorescence

HeLa cultured cells were fixed with 4% paraformaldehyde. Dako REAL Antibody Diluent was used for blocking for 10 minutes at room temperature. Primary antibodies were incubated for 2 hours at room temperature (anti-TRIP Abcam 151307, anti-TRIP Abcam 4533, anti-FLAG Sigma F7425).

Immunohistochemistry

Five μm sections were cut from formalin-fixed, paraffin-embedded tissue block, placed on glass slide and dried out at 30° during 3 hours. Sections were deparaffinized in xylene and rehydrated in ascending grades of alcohol. Antigen retrieval was performed in pH 6 Citrate buffer 1M at 95° for 15 minutes, using a microwave. In some cases, pH 9 Tris 10 mM-EDTA 1,26 mM at 95° during 20 minutes was preferred. Endogenous peroxidase activity was exhausted by incubation of tissue sections in 3% hydroxide peroxide for 10 minutes. 2,5% ready-to use horse serum from ImmPRESS anti-rabbit (Vector laboratories) was used for blocking. The primary antibody was the Abcam 151307. It was diluted at 1:1500 in 2,5 % ready-to-use horse serum at room temperature for 1 hour. Slides were then incubated with a ready to use secondary antibody (ImmPRESS anti-rabbit, Vector laboratories) for 30 minutes at room temperature. The antigen-antibody complex was visualized with the chromogen DAB which was incubated for 5 minutes and counterstained with hematoxylin. All tissue sections were stained under similar conditions to ensure equal staining quality. A negative control was performed in all cases by omitting the primary antibody, which in all instances resulted in negative immunoreactivity.

Pictures were taken by AxioCam and AxioVision software 4.8. Images were analyzed by ImageJ and IHC Profiler.

5 BIBLIOGRAPHY

1. Lee SYS, Choi YY. TRAF-interacting protein (TRIP): a novel component of the tumor necrosis factor receptor (TNFR)- and CD30-TRAF signaling complexes that inhibits TRAF2-mediated NF-kappaB activation. *Journal of Experimental Medicine*. 1997 Apr 6;185(7):1275–85.
2. Besse AA, Campos ADA, Webster WKW, Darnay BGB. TRAF-interacting protein (TRIP) is a RING-dependent ubiquitin ligase. *Biochem Biophys Res Commun*. 2007 Aug 2;359(3):5–5.
3. Berndsen CE, Wolberger C. New insights into ubiquitin E3 ligase mechanism. *Nature Structural & Molecular Biology*. Nature Publishing Group; 2014 Apr 1;21(4):301–7.
4. Spasser L, Brik A. Chemistry and Biology of the Ubiquitin Signal. *Angew Chem Int Ed*. 2012 Jun 13;51(28):6840–62.
5. Satija YK, Bhardwaj A, Das S. A portrayal of E3 ubiquitin ligases and deubiquitylases in cancer. *Int J Cancer*. 2013 Mar 25;1–10.
6. Chapard C, Hohl D, Huber M. The role of the TRAF-interacting protein in proliferation and differentiation. *Experimental Dermatology*. 2012 Apr 18;21(5):321–6.
7. Wallace HA, Merkle JA, Yu MC, Berg TG, Lee E, Bosco G, et al. TRIP/NOPO E3 ubiquitin ligase promotes ubiquitylation of DNA polymerase. *Development*. 2014 Mar 4;141(6):1332–41.

8. Zhang MM, Wang LL, Zhao XX, Zhao KK, Meng HH, Zhao WW, et al. TRAF-interacting protein (TRIP) negatively regulates IFN- β production and antiviral response by promoting proteasomal degradation of TANK-binding kinase 1. *Journal of Experimental Medicine*. 2012 Sep 23;209(10):1703–11.
9. Merkle JA, Rickmyre JL, Garg A, Loggins EB, Jodoin JN, Lee E, et al. no poles encodes a predicted E3 ubiquitin ligase required for early embryonic development of *Drosophila*. *Development*. 2009 Jan 13;136(3):449–59.
10. Almeida SS, Ryser SS, Obarzanek-Fojt MM, Hohl DD, Huber MM. The TRAF-interacting protein (TRIP) is a regulator of keratinocyte proliferation. *CORD Conference Proceedings*. 2011 Jan 31;131(2):349–57.
11. Chopard C, Meraldi P, Gleich T, Bachmann D, Hohl D, Huber M. TRIP is a regulator of the spindle assembly checkpoint. *Journal of Cell Science*. The Company of Biologists Ltd; 2014 Dec 15;127(24):5149–56.
12. Regamey AA, Hohl DD, Liu JWJ, Roger TT, Kogerman PP, Toftgard RR, et al. The tumor suppressor CYLD interacts with TRIP and regulates negatively nuclear factor kappaB activation by tumor necrosis factor. *Journal of Experimental Medicine*. 2003 Dec 14;198(12):1959–64.
13. Bignell GR, Warren W, Seal S, Takahashi M, Rapley E, Barfoot R, et al. Identification of the familial cylindromatosis tumour-suppressor gene. *Nat Genet*. 2000 Jun;25(2):160–5.
14. Kuphal S, Shaw-Hallgren G, Eberl M, Karrer S, Aberger F, Bosserhoff AK, et al. GLI1-dependent transcriptional repression of CYLD in basal cell carcinoma. *Oncogene*. 2011 Nov 2;30(44):4523–30.
15. Massoumi RR, Chmielarska KK, Hennecke KK, Pfeifer AA, Fässler RR. Cyld Inhibits Tumor Cell Proliferation by Blocking Bcl-3-Dependent NF- κ B Signaling. *Cell*. 2006 May 18;125(4):13–3.
16. Alameda JP, Fernández-Aceñero MJ, Moreno-Maldonado R, Navarro M, Quintana R, Page A, et al. CYLD regulates keratinocyte differentiation and skin cancer progression in humans. *Cell Death Dis*. 2011;2:e208.
17. Zhou Q, Geahlen RL. The protein-tyrosine kinase Syk interacts with TRAF-interacting protein TRIP in breast epithelial cells. *Oncogene*. 2009 Mar 11;28(10):1348–56.
18. Kasper M, Jaks V, Hohl D, Toftgard R. Basal cell carcinoma — molecular biology and potential new therapies. *J Clin Invest*. 2012 Feb 1;122(2):455–63.
19. Sexton M, Jones DB, Maloney ME. Histologic pattern analysis of basal cell carcinoma. Study of a series of 1039 consecutive neoplasms. *Journal of American Dermatology*. 1990 Dec;23(6 Pt 1):1118–26.
20. Grachtchouk V, Grachtchouk M, Lowe L, Johnson T, Wei L, Wang A, et al. The magnitude of hedgehog signaling activity defines skin tumor phenotype. *The EMBO Journal*. 2003 Jun 2;22(11):2741–51.
21. Freier K, Flechtenmacher C, Devens F, Hartschuh W, Hofele C, Lichter P, et al. Recurrent NMYC copy number gain and high protein expression in basal cell carcinoma. *Oncol Rep*. 2006 May;15(5):1141–5.
22. Yu M, Zloty D, Cowan B, Shapiro J, Haegert A, Bell RH, et al. Superficial, Nodular, and Morpheiform Basal-Cell Carcinomas Exhibit Distinct Gene Expression Profiles. *J Invest Dermatol*. 2008 Jan 17;128(7):1797–805.
23. Ratushny V, Gober MD, Hick R, Ridky TW, Seykora JT. From keratinocyte to cancer: the pathogenesis and modeling of cutaneous squamous cell carcinoma. *J Clin Invest*. 2012 Feb 1;122(2):464–72.
24. Martorell-Calatayud A, Sanmartín Jimenez O, Cruz Mojarrieta J, Guillén Barona C. Cutaneous Squamous Cell Carcinoma: Defining the High-Risk Variant. *Actas Dermo-Sifiliográficas (English Edition)*. 2013 Jun;104(5):367–79.
25. Livak KJ, Schmittgen TD. Analysis of Relative Gene Expression Data Using Real-Time Quantitative PCR and the 2- $\Delta\Delta$ CT Method. *Methods*. 2001 Dec;25(4):402–8.
26. Minner F, Poumay Y. Candidate housekeeping genes require evaluation before their selection for studies of human epidermal keratinocytes. *J Invest Dermatol*. 2009 Mar;129(3):770–3.
27. Bär M, Bär D, Lehmann B. Selection and Validation of Candidate Housekeeping Genes for Studies of Human Keratinocytes—Review and Recommendations. *J Invest Dermatol*. 2009 Mar;129(3):535–7.
28. Sullivan CAW, Chung GG. Biomarker Validation: In Situ Analysis of Protein Expression Using Semiquantitative Immunohistochemistry-Based Techniques. *Clinical Colorectal Cancer*. Elsevier Inc; 2011 Jul 28;7(3):172–7.

29. Bordeaux J, Welsh A, Agarwal S, Killiam E, Baquero M, Hanna J, et al. Antibody validation. *BioTechniques*. 2010 Mar;48(3):197–209.
30. Taylor CR, Levenson RM. Quantification of immunohistochemistry--issues concerning methods, utility and semiquantitative assessment II. *Histopathology*. 2006 Oct;49(4):411–24.
31. Rizzardi AE, Johnson AT, Vogel RI, Pambuccian SE, Henriksen J, Skubitz AP, et al. Quantitative comparison of immunohistochemical staining measured by digital image analysis versus pathologist visual scoring. *Diagn Pathol*. BioMed Central Ltd; 2012;7(1):42.
32. Parker AS, Lohse CM, Leibovich BC, Cheville JC, Sheinin YM, Kwon ED. Comparison of digital image analysis versus visual assessment to assess survivin expression as an independent predictor of survival for patients with clear cell renal cell carcinoma. *Human Pathology*. 2008 Aug;39(8):1176–84.
33. Turbin DA, Leung S, Cheang MCU, Kennecke HA, Montgomery KD, McKinney S, et al. Automated quantitative analysis of estrogen receptor expression in breast carcinoma does not differ from expert pathologist scoring: a tissue microarray study of 3,484 cases. *Breast Cancer Res Treat*. 2007 Oct 3;110(3):417–26.
34. Ong CW, Kim LG, Kong HH, Low LY, Wang TT, Supriya S, et al. Computer-assisted pathological immunohistochemistry scoring is more time-effective than conventional scoring, but provides no analytical advantage. *Histopathology*. 2010 Mar;56(4):523–9.
35. Feuchtinger A, Stiehler T, Jütting U, Marjanovic G, Luber B, Langer R, et al. Image analysis of immunohistochemistry is superior to visual scoring as shown for patient outcome of esophageal adenocarcinoma. *Histochem Cell Biol*. 2015 Jan;143(1):1–9.
36. Bertheau P, Cazals-Hatem D, Meignin V, de Roquancourt A, Vérola O, Lesourd A, et al. Variability of immunohistochemical reactivity on stored paraffin slides. *J Clin Pathol*. 1998 May;51(5):370–4.
37. Mudduwa L, Liyanage T. Immunohistochemical assessment of hormone receptor status of breast carcinoma : Interobserver variation of the quick score. *Indian J Med Sci*. 2009;63(1):21.
38. Varghese F, Bukhari AB, Malhotra R, De A. IHC Profiler: an open source plugin for the quantitative evaluation and automated scoring of immunohistochemistry images of human tissue samples. *PLoS ONE*. 2014;9(5):e96801.
39. Walker RA. Quantification of immunohistochemistry--issues concerning methods, utility and semiquantitative assessment I. *Histopathology*. 2006 Oct;49(4):406–10.